PRESSURE INDICATORS FOR MEASUREMENTS IN WIND TUNNELS

L. B. Nevskii and S. M. Zadonskii

UDC 533.6.071.082.5

The results of an investigation of new materials sensitive to air pressure in a given pressure range are reported. Examples of their application to wind tunnels are given.

The materials developed may be used as a thin film with a thickness of about 10 μm sprayed onto a surface of aerodynamic models with the help of an aerograph. These films represent pressure indicators. The indicator films possess satisfactory adhesion and are nontoxic.

Original information on the development and application of the pressure indicators is given in [1-3]. The present paper offers some information concerning further research and improvement of the indicators. The very idea of their application is of great interest because such indicators allow quick measurement of the pressure distribution over the surface of aerodynamic models at any point and construction surfaces of the measured values.

After spray-deposition, the model is only dried for several minutes and is already ready for measurements. The measurements at a great number of points by the known drainage method require several months for a pre-starting procedure.

The indicator method is based on application of luminophors, the intensity of retarded fluorescence (RF) of which depends on the oxygen pressure. An increase of the pressure leads to RF quenching. RF excitation is accomplished by an impulse light source, then photographing is done and the optical density of photofilm blackening is measured by a microdensitometer. The blackening density is proportional to the measured pressure. Calibration is performed prior to or after wind-tunnel testing at the same model temperature without a flow and in a flow. For this, several air pressure values are set in succession in a working chamber without a flow. This is the first calibration technique. Calibration may also be performed against two points on the model surface with a known pressure at a constant temperature over the model surface. This is the second calibration technique. In the latter case, two drainage holes are made at convenient places on the model surface, or these two pressure values are determined theoretically.

The measurement time must be short because of the high cost associated with starting the wind tunnel. The time of measurement by the indicator technique is determined by RF duration and the time of determination of the air concentration distribution in an indicator film proportional to the measured pressure. The RF intensity, ensuring normal optical density of photofilm blackening in our recording equipment, is attained at 2 sec from the moment of flash of the impulse light source at an air rarefaction of 10^4 Pa. Determination of the air concentration distribution takes much more time (the relaxation time). It determines, in essence, the measurement duration. The relaxation time depends on the air pressure and oxygen permeability of an indicator film related with oxygen diffusion. For the purpose of elucidation, it is sufficient to confine the discussion to a one-dimensional diffusion boundary and solve the following boundary-value problem

$$C_t = a^2 C_{xx},\ 0 < x < \infty,\ 0 < t < \infty,$$
$$C(x,\ 0) = 0,\ C(0,\ t) = C_0(t).$$

Here $a^2 = D_c/n = r_1^2 C_1 RT/(8\eta n)$ [4].

Integration yields the equation

$$C(x,\ t) = C_0(t)\left(1 - x(8n\eta)^{1/2}/r_1(\pi C_1 RTt)^{1/2}\right), \tag{1}$$

from which it is seen that with decreasing porosity, C(x, t) increases, the relaxation time decreases. With increasing C_1, C(x, t) increases but the relaxation time also decreases. Therefore in subsonic and transonic flows with a small degree of rarefaction, the relaxation time is small, while for supersonic flows with a high degree of rarefaction of an incoming flow, it increases.

Central Aero-Hydrodynamics Institute, Moscow. Translated from Inzhenerno-Fizicheskii Zhurnal, Vol. 63, No. 2, pp. 183-187, August, 1992. Original article submitted October 25, 1990.

1062-0125/92/6302-0795$12.50

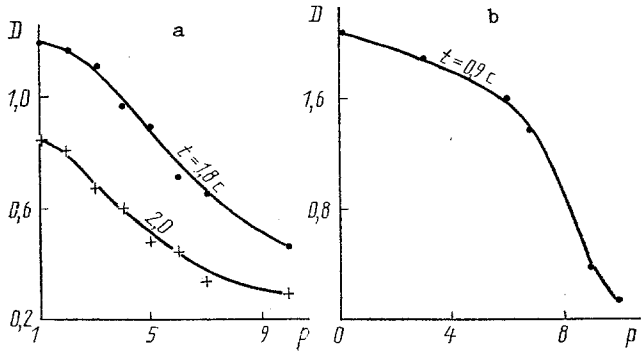

Fig. 1. Optical density of photofilm blackening vs air pressure at photographing of indicators: a) for the first indicator; p, 10^3 Pa; b) for the second indicator; p, 10^4 Pa.

The relaxation time was measured on a vacuum bench, with air evacuated out of the hood of the device. At a fixed pressure, RF was photographed in certain time intervals and the time at which D values became constant was determined. For our indicator with a matrix consisting of finely ground silica gel and oxygen-permeable starch, the relaxation time lasted 5 min at an air pressure of $2 \cdot 10^3$ Pa. In contradiction with the requirement to decrease the relaxation time is the requirement to decrease smearing of a useful signal. For instance, instead of a thin line of a shock wave, a broad band may be obtained. To decrease the signal smearing, we must decrease the diffusion. For this, the specific surface connected with porosity must be larger, for instance, 100-140 m^2/g, while the pore radius must be smaller, e.g., 10-15 nm. Smearings will be more pronounced in a film with a specific surface, for example, of 5-15 m^2/g and a pore radius of 50-70 nm. The dependence of C(x, t) on the pore radius is determined in Eq. (1). To match these two contradictory requirements, it is necessary to choose the appropriate material. We consider the influence of the temperature and sensitivity of a recording device. The intensity of retarded fluorescence without taking account of an indicator film thickness, nonuniformity of film painting with luminophor, photofading, dimerization, concentration quenching, and mole fraction of oxides is as follows:

$$I = I_0 \exp\left(-(KC\tau_0 + 1)\, t/\tau_0\right), \tag{2}$$

$$K = q \langle v \rangle \sigma N_0, \tag{3}$$

$$\langle v \rangle = (8kT/\pi m)^{1/2}, \tag{4}$$

$$C = C_0 (p/p_0)^{RT/E}.$$

The complete expression for I is given in [3]. If we use additionally the known formula

$$\lg I/I_0 = (D - D_0)/\gamma \tag{5}$$

and write relations (2)-(5) for the points 1, 2, i, then we obtain

$$p_i^* = p_i/p_\infty y = a_1 + a_2 (D_i - D_{0i}), \tag{6}$$

$$a_1 = p_1^* + D_1 p_1^* / ((D_2 - D_1)\, c_2 T)\, (1 - (p_2^*/p_1^*)^{c_2 T}),$$

$$a_2 = p_1^* / ((D_1 - D_2)\, c_2 T)\, (1 - (p_2^*/p_1)^{c_2/T}),$$

$$c_2 = R/E, \quad i = 3, 4, \ldots$$

for constant temperature T. The coefficients a_1 and a_2 are found at calibration. From (6) follows the temperature constancy of the model without a flow and in a flow for the first calibration technique and the temperature constancy over the model surface in a flow at the second calibration technique. Temperature quenching of RF depends on the pressure of the matrix into which the luminophor is placed and on the time, during which the excited luminophor molecules are exposed to the temperature. Organic luminophor quenching in a silica gel matrix at an air pressure of $9.8 \cdot 10^4$ Pa in the temperature range 278-298 K

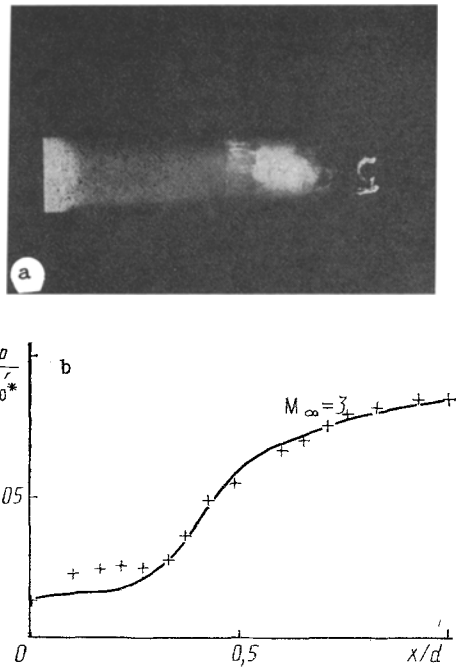

Fig. 2. Photo of RF on the cylinder (a) and measurement results (b): points) the indicator method; curve) the drainage method.

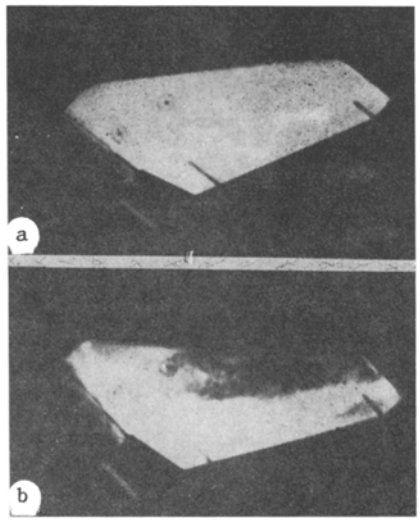

Fig. 3. Photo of RF on a vertical airplane tail surface.

attains a maximum value of 40%. At $3.9 \cdot 10^4$ Pa and the same temperature range, the quenching is 3% at one and the same t. This circumstance favors application of the indicators in wind tunnels since at supersonic velocities on side surfaces of aerodynamic models the pressure does not exceed $3.9 \cdot 10^4$ Pa. If duralumin models are used, temperature gradients after model heating in a flow make up a few degrees. But this cannot exert a pronounced influence on I. Here it is implied that an incoming flow is not heated. For subsonic and transonic flows, the pressure on a side surface is about $8.8 \cdot 10^4$ Pa or lower, but the model is not being heated and temperature gradients on metallic models are, in fact, absent. At $9.8 \cdot 10^4$ Pa and the temperature range 283-299 K, the maximum luminophor quenching in a polymer matrix makes up 45%, while in a silica gel matrix it equals 36% at a time of temperature effect on the excited molecules being t = 2 sec. For the indicator with a silica gel matrix activated, for instance, by beta-amino-anthraquinone, the maximum quenching is 4% at t = 0.5 sec for the same temperature range.

A decrease of the temperature quenching by introducing active dopants, e.g., salt LiI [5], actually does not occur.

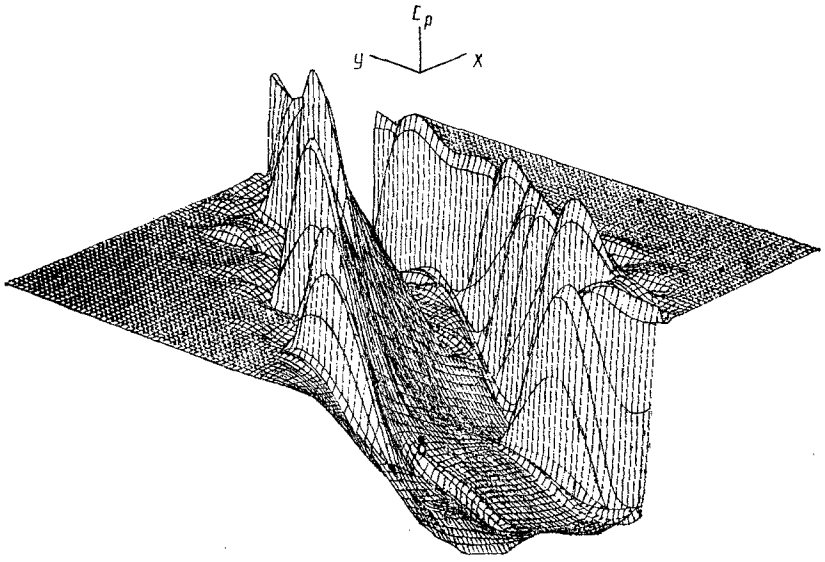

Fig. 4. Surface of pressure coefficients C_p for a vertical airplane tail surface at $M_\infty = 3$, $\alpha = 22.5°, \beta = +1°$.

Now we move to the sensitivity of a recording device. At a correct choice of luminophor concentration in a film, no concentration quenching and dimerization take place. In this case, the sensitivity is

$$M = dD/dp = \gamma \lg etKr \exp(-((1 - m_0 I_0 (1 - 10^{-k' l/c_2})) + Kr\tau_0 p)\, t/\tau_0). \quad (7)$$

In the absence of light overabsorption in an indicator film, Eq. (7) has no Bouguer–Lambert–Beer correction, and we can write

$$M = \gamma \lg eb \exp(-(1 + bp)\, t/\tau_0)\, t/\tau_0.$$

As is seen, sensitivity depends highly on t. Indeed, in the course of time, an experimenter can observe the pressure distribution on the model in detail. Then this picture disappears as far as the luminophor molecules become deactivated. The maximum sensitivity is determined from the equation

$$dM/d(t/\tau_0) = 0$$

and is attained for the time

$$t/\tau_0 = 1/(1 + bp).$$

Whence it follows that with increasing p, t/τ_0 increases, i.e., the device sensitivity increases. In this case, the possibility exists of using this method in vacuum tubes.

Figure 1a represents the lines D = D(p) for the air pressure range 10^3-10^4 Pa at t = 1.8 and 2.0 sec for an indicator with a finely ground silica gel matrix and oxygen-permeable starch for the first indicator. Here, the pressure difference at two points may be resolved by the value 150-300 Pa. Figure 1b shows the line D = D(p) for the range 10^3-10^5 Pa at t = 0.9 sec for an indicator with a matrix consisting of two polymers. This is the second indicator. One polymer is oxygen-permeable, while other is oxygen-impermeable. Varying the content of these polymers in the matrix, we may obtain indicators for different pressure ranges. The second indicator is intended to measure transonic air flows. The indicator sensitivity in the range $6 \cdot 10^4$-10^5 Pa is $0.2 \cdot 10^4$ Pa^{-1}. The resolving power is 10^3 Pa.

Figure 2a is a photo of retarded fluorescence on a cylinder with a plane face at $M_\infty = 3$ for an indicator with a matrix consisting of ground silica gel with the addition of an oxygen-impermeable polymer. The light region on the cylinder is the result of rarefaction behind a head shock wave, which entraps the front section of the model. Figure 2b shows the result of quantitative processing. The solid line of pressure p/p_{0*}' is obtained by the known drainage method of pressure measurement. Discrete points are found by the indicator method. For this, formula (6) is used. The origin of the x/d axis is on the cylinder face. The x/d coordinate is directed along the axis of symmetry of the cylinder. The standard deviation of the indicator points from the

drainage ones is about 15%. Indicator measurements performed on different bodies at a supersonic speed and on wing lines at a transonic speed are made by the present authors with a root-mean-square error of 6-12%.

Figure 3 is a photo of retarded fluorescence on the vertical tailplane of an airplane at $M_\infty = 0$ (a) and $M_\infty = 3$ (b) at an angle of slide $\beta = +1^0$. Figure 4 shows the surface of pressure coefficients C_p for this tailplane. The origin of the coordinates is on the leading edge of the vertical tailplane on the line of conjugation with the fuselage. The x axis is parallel to the airplane axis. Measurements are made in the sections y = const.

As is seen, the pressure coefficients near the leading edge of a vertical tailplane increase with increasing y coordinate, i.e., in the direction from the fuselage surface. Such a pressure distribution in the region of the leading edge is consistent with a representation of flow field on the lee side of an aircraft for supersonic velocities of the flow at large angles of attack. Along the vertical tailplane chord, the flow broadening is observed. Thus, pressure indicators give more complete information about air pressure distribution on the surface of aerodynamic models, as compared with the drainage method, which allows investigation of more delicate aerodynamic effects. Obtaining of such information requires less time. The chemical compositions of the pressure indicators are given in [6].

NOTATION

C, oxygen concentration proportional to measured pressure; D_c, diffusion coefficient; n, porosity coefficient of an indicator film; x, coordinate; r_1, pore radius; C_1, total oxygen concentration; R, gas constant; T, absolute temperature; η, oxygen viscosity; D, optical density of blackening; $\langle v \rangle$, mean Maxwellian velocity of oxygen molecules; σ, area of a luminescent molecule; q, quenching probability at collision of an oxygen molecule with a luminescent molecule; N_0, Avogadro number; k, Boltzmann constant; m, oxygen molecule mass; E, characteristic energy of oxygen solubility in an indicator film; I_0, intensity of retarded fluorescence (RF) at t = 0; D_0, optical density of blackening for I_0; γ, protofilm gamma; p_∞, static pressure of an incident air flow; y, molar fraction of oxygen in air; D_i, optical density of photofilm blackening for the model in the flow at the point i; D_{0i}, optical density of photofilm blackening for the model without the flow at the point i; p_i^*, air pressure based on pressure p_* at the point i; t, diffusion time or time between flash of an impulse light source and opening of a camera shutter plus exposure time; e = 2.718; K, rate constant of a bimolecular reaction between excited luminophor molecules and oxygen molecules; r, Henry coefficient or oxygen permeability coefficient of a film; m_0, constant; I_0, initial RF intensity; k′, constant; c_2, concentration of unexcited luminophor molecules in a film; l, film thickness; τ_0, lifetime of excited luminophor molecules at the oxygen pressure p = 0, $b = Kr\tau_0$; M_∞, Mach number of incoming flow; $p'_0{}^*$, air pressure at the stagnation point on the model nose; C_p, pressure coefficient; d, cylinder diameter.

LITERATURE CITED

1. M. M. Ardasheva, L. B. Nevskii, and G. E. Pervushin, Zh. Prikl. Mekh. Tekh. Fiz., No. 4, 24-30 (1985).
2. L. B. Nevskii, G. E. Pervushin, and G. I. Sidel'nikova, Uch. Zap. TsAGI, **21**, No. 1, 98-104 (1990).
3. L. B. Nevskii, "Development of optical methods of visualization and determination of gas flow parameters," Candidate's Dissertation (Engineering), Moscow (1986).
4. V. S. Komarov, Adsorbents and Their Properties [in Russian], Minsk (1977).
5. V. V. Bryukhanov, L. V. Levshin, Zh. K. Smagulov, and Z. M. Muldalhmetov, Zh. Prikl. Spektrosk., **44**, No. 3, 393-397 (1986).
6. Inventor's Certificate 1065452 USSR: ICI C 09D5/00. The Composition for an Indicator Coating (Its Variants).